

Optimization of bio-oil production parameters from the pyrolysis of elephant grass (*Pennisetum purpureum*) using response surface methodology

Sunday C. Ikpeseni^{1*}, Samuel O. Sada¹, Ufuoma J. Efetobor^{1,2}, Henry O. Orugba³, Mathias Ekpu¹, Hilary I. Owamah⁴, Jeremiah L. Chukwunke⁵, Solomon Oyebisi^{6,7} and Uche P. Onochie⁸

¹Department of Mechanical Engineering, Delta State University, P.M.B. 1, Abraka, Nigeria

²Department of Mechanical Engineering, Delta State Polytechnic, P.M.B. 3, Otefe-Oghara, Nigeria

³Department of Chemical Engineering, Delta State University, P.M.B.1, Abraka, Nigeria

⁴Department of Civil Engineering, Delta State University, P.M.B. 1, Abraka, Nigeria

⁵Department of Mechanical Engineering, Nnamdi Azikiwe University, P.M.B. 2025, Awka, Nigeria

⁶Department of Civil Engineering, Covenant University, P.M.B. 1023, Otta, Nigeria

⁷Department of Civil Engineering, The University of the South Pacific, P.M.B. 9072, Suva, Fiji

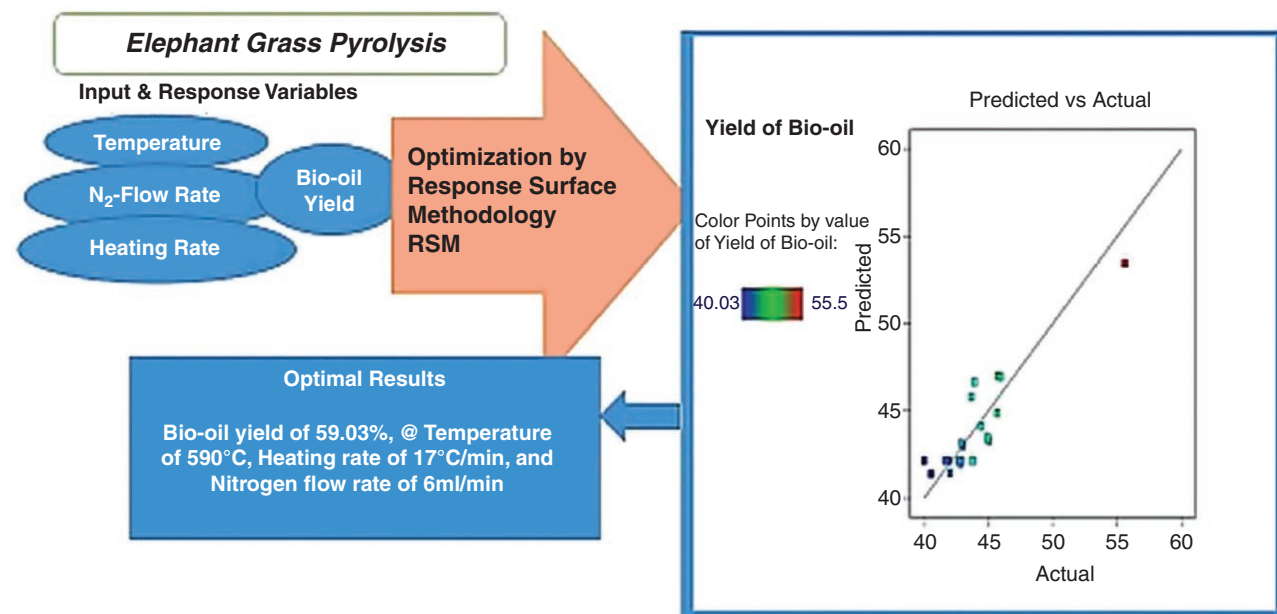
⁸Department of Mechanical Engineering, Delta State University of Science and Technology, P.M.B. 5, Ozoro, Nigeria

*Corresponding author. E-mail: scikpeseni@delsu.edu.ng

Abstract

The need to increase bio-oil yield from biomass and enhance its fuel properties has driven research into optimizing the pyrolysis process. This study investigated the influence of three key process parameters—temperature, heating rate, and nitrogen flow rate—on the pyrolysis of elephant grass (*Pennisetum purpureum*) in a fixed-bed reactor. Response surface methodology was used to study the impact of the aforementioned variables on bio-oil yield to improve its production efficiency. Proximate analysis of the biomass revealed 79.24 wt% volatile matter, 14.22 wt% fixed carbon, and 5.86% ash, with ultimate analysis showing 45.44% carbon, 5.59% hydrogen, and 40.95% oxygen. The high volatile matter content and favourable carbon and hydrogen percentages indicate that elephant grass is a viable energy source due to its potential for high bio-oil yield and energy content. The resulting bio-oil exhibited a higher heating value of 20.9 MJ/kg, indicating its suitability for various heating applications. A second-order regression model was developed for bio-oil yield, with optimal conditions identified as a temperature of 550°C, a heating rate of 17°C/min, and a nitrogen flow rate of 6 ml/min. The study achieved an optimal bio-oil yield of 59.03 wt%, and the model's high R^2 value of 0.8683 from analysis of variance analysis confirmed its predictive accuracy. This research highlights elephant grass as a sustainable feedstock for bio-oil production, offering valuable insights into optimizing pyrolysis conditions to enhance bio-oil yield, thus advancing biofuel technology.

Graphical abstract



Received: 23 April 2024. Accepted: 2 August 2024

© The Author(s) 2024. Published by Oxford University Press on behalf of National Institute of Clean-and-Low-Carbon Energy

This is an Open Access article distributed under the terms of the Creative Commons Attribution License (<https://creativecommons.org/licenses/by/4.0/>), which permits unrestricted reuse, distribution, and reproduction in any medium, provided the original work is properly cited.

Keywords: renewable energy; biomass; sustainable feedstock; regression model; fixed-bed reactor

1. Introduction

Biomass has been identified as a suitable supplement for the fast-depleting conventional fuel resources and an eco-friendly alternative capable of playing important roles in future energy systems [1]. To reduce environmental pollution caused by the release of greenhouse gas emissions (GHGs) from fossil fuel usage [2], different conversion schemes have been developed over the years to convert biomass into biofuel for use in many combustion systems. The transformation of biomass into biofuel can be achieved via physical, biological, biochemical, or thermochemical processes. Pyrolysis, the thermochemical transformation of biomass into energy, has gained wide interest due to its benefits and flexibility, and many studies have revealed it as one of the most efficient biomass-to-biofuel conversion technologies [3–6].

The pyrolysis of biomass produces bio-oil, bio-char, and syngas; the most valuable of the products is bio-oil [7]. Although pyrolysis-derived bio-oil has various potential applications, such as energy production, fuels, chemicals, and carbon materials [8], the direct use of bio-oil is limited in many systems due to some undesirable characteristics like its corrosive nature, high acidity, instability at room temperature, and low heating value [9, 10]. In order to enhance the quality of the bio-oil, it is usually subjected to different upgrading techniques. The yield and quality of the bio-oil have been linked to reactor type, the intrinsic transport process, and the right combination of process parameters during pyrolysis [11]. Therefore, it is imperative that the right combination of pyrolysis processing parameters for optimum bio-oil yield be obtained using suitable optimization techniques. This study applied response surface methodology (RSM) to determine the optimal bio-oil yield from the fast pyrolysis of elephant grass.

RSM aids in identifying optimal conditions by efficiently optimizing multiple variables, understanding complex relationships, reducing experiments, providing statistical analysis, visualizing response surfaces, and ensuring robustness and reliability in experimental setups [12–14]. RSM has been effectively utilized across various studies to optimize bio-oil production from biomass pyrolysis. Balamurugan et al. [15] used RSM to optimize transesterification parameters for biodiesel production from mixed non-edible oils, achieving high yields of up to 95.91%. Oyebanji et al. [16] studied the catalytic pyrolysis of wood sawdust using RSM, employing a green zeolite-Y catalyst synthesized from *Ficus exasperata* (L.) leaf particles. They identified an optimal biomass-to-catalyst ratio of 80/20% and a reaction temperature of 550°C, leading to a significant increase in pyrolytic liquid yield. Onokwai et al. [17] optimized the pyrolysis of sugarcane bagasse using RSM, determining key parameters such as a temperature of 493.7°C, a reaction time of 15.5 min, a heating rate of 24.5°C/min, a nitrogen flow rate of 225 cm³/min, and a particle size of 0.1 mm. This study resulted in bio-oil enriched with alkenes, alcohols, esters, and other valuable compounds suitable for various industrial applications. Jeeru et al. [18] investigated the pyrolysis of algal biomass in a batch fixed-bed reactor, applying RSM to optimize temperature, retention time, and nitrogen flow rate. They achieved a maximum bio-oil yield at 575°C, a 45-min retention time, and a nitrogen flow rate of 0.5 l/min, with the bio-oil containing compounds like 4-methylpentanamide and *n*-heptadecane. Fombu et al. [19] conducted pyrolysis of cashew nut shells using RSM to maximize bio-oil yield in a fixed-bed reactor, achieving a notable liquid yield of 61.3 wt%. Their approach

demonstrated the efficacy of RSM compared to traditional one-factor-at-a-time experiments, which yielded 57.8%. Irfan et al. [20] utilized RSM to optimize bio-oil production from rice husk ash, achieving a maximum yield of 20.33% at 480°C with a heating rate of 80°C/min and a particle size of 200 μm. The upgraded bio-oil exhibited desirable properties such as a density of 0.98 g/cm³ and an acid value of 58 mg KOH/g, enhancing its potential for various applications.

One of the most abundant but under-explored biomasses is elephant grass (*Pennisetum purpureum*). Elephant grass is an excellent biomass source for bioenergy due to its non-food crop nature and broad availability. Elephant grass can thrive in various climates and, exhibiting rapid growth, can produce high dry matter yields of 40–41 t/ha over 260 days, surpassing the biomass yield of other energy grasses [21]. Its robust growth and ability to flourish on infertile lands make it ideal for both livestock feeding and energy production without competing with food crops for arable land. While elephant grass serves as an important forage crop for livestock, its robust stalks are often overlooked for animal feeding due to their lower nutritional value and digestibility compared to the younger leaves [22]. However, these stalks possess significant potential as a bioenergy feedstock, owing to their high cellulosic fibre content, which makes them an ideal resource for sustainable energy practices [23]. The pyrolysis process of elephant grass generates high-quality bio-oil and valuable by-products such as bio-char, which is useful for soil enhancement and carbon sequestration, as well as syngas, which can be used for heat generation, underscoring its significant potential in bioenergy applications [23–26].

In the fast pyrolysis of elephant grass, according to the available literature, the tailored optimization of the three key process variables—temperature, heating rate, and nitrogen flow rate—to maximize bio-oil yield with enhanced fuel properties remains a notable research gap in biomass pyrolysis. This research specifically aims to optimize the pyrolysis process to maximize bio-oil yield from this novel feedstock. Central composite design (CCD) of RSM was chosen for its efficiency, ability to capture variable interactions, and effectiveness in optimizing multi-parameter processes. The indicator used, bio-oil yield, was chosen to directly measure the efficiency of the pyrolysis process in converting biomass into valuable liquid fuel. These choices align with the study's goals and offer significant advantages over other potential models and materials.

2. Materials and methods

2.1 Sample preparation

Fresh elephant grass samples obtained from a farm in Oghara, Delta State, Nigeria, were cleaned to remove impurities and chopped for size reduction. The samples were sun-dried for 5 days [23]. Subsequently, the dried samples were pulverized in a ball mill, sieved to an average particle size of 0.2 mm, and stored in Ziploc bags at room temperature.

2.2 Characterization of biomass and bio-oil

Various characterization techniques were used to analyse the biomass and its bio-oil. The proximate analysis of the elephant grass, following the American Society of Testing and Materials (ASTM) methods outlined in Isahak et al. [27], measured volatile

matter, moisture content, fixed carbon, and ash content. The ultimate analysis, using a LECO CHN 2000 elemental analyser, determined the nitrogen, carbon, hydrogen, and sulphur contents, with the oxygen content calculated by difference. The structural composition of the biomass, including cellulose, hemicelluloses, and lignin, was assessed according to the ASTM standard outlined by Onarheim *et al.* [28]. The physico-chemical and fuel properties of the resulting bio-oil were analysed, and its functional groups were identified using Fourier transform infrared (FTIR) spectroscopy (Perkin-Elmer 100). A small drop of the bio-oil was placed between two potassium bromide (KBr) discs and pressed into a pellet for the FTIR analysis. The sample was then placed in the FTIR spectrometer, and the infrared spectrum was recorded in the range of 4000–600 cm^{-1} , revealing the absorption bands corresponding to various functional groups present in the bio-oil.

To examine the chemical composition of the bio-oil, gas chromatography-mass spectrometry (GC-MS) (Agilent 7890 GC/5975 MS) was used. The bio-oil sample was diluted with dichloromethane and filtered. A small drop of the diluted sample was injected into the gas chromatograph (GC), where the compounds were separated based on their boiling points and interactions with the stationary phase in the GC column. The separated compounds were then ionized and detected by the mass spectrometer (MS), providing information about their molecular weights and fragmentation patterns. The GC-MS data were pro-

cessed using software to identify the individual compounds by comparing their mass spectra with reference libraries or databases.

2.3 Pyrolysis experiments

Bio-oil was produced from elephant grass using a pyrolysis system with a fixed-bed reactor. The reactor has a bed depth of 50 mm and a mass flow rate of 1 kg/h. Each pyrolysis experiment was performed for 5 s. The reactor has a bed depth of 50 mm, mass flowrate of 1 kg/h and the pyrolysis was performed for 5 s. Following the experimental procedures outlined in Table 2, 20 g of biomass was weighed and fed into the reactor. The reactor was purged with nitrogen supplied at a predetermined flow rate and operated for 25 min. During the process, the bio-oil was recovered as condensed vapours from the condenser, while the uncondensed gaseous products were flared off. At the end of each reaction, the char was removed from the reactor. The recovered bio-oil was then weighed using a mass balance, and the percentage yield was calculated using Equation (1). The yields of bio-char and syngas were also calculated using Equations (2) and (3), respectively [23],

$$\text{Bio-oil yield (\%)} = \frac{\text{Mass of bio-oil (g)}}{\text{Mass of elephant grass biomass (g)}} \times 100 \quad (1)$$

$$\text{Bio-char yield (\%)} = \frac{\text{Mass of bio-char (g)}}{\text{Mass of elephant grass biomass (g)}} \times 100 \quad (2)$$

$$\text{Syngas yield (\%)} = 100 - (\text{Bio-oil yield} + \text{Bio-char yield}) \quad (3)$$

2.4 Experimental design

Using CCD of RSM, the bio-oil yield was optimized. The independent variables—pyrolysis temperature, nitrogen flow rate, and heating rate—were investigated at four levels. The number of experiments, n , was determined from Equation (4):

Table 1. Ranges of variables used.

Factor/unit	Symbol	Range	
		High	Low
Temp. ($^{\circ}\text{C}$)	<i>I</i>	750	350
Heating rate ($^{\circ}\text{C}/\text{min}$)	<i>J</i>	20	5
N_2 flowrate (ml/min)	<i>K</i>	8	2

Table 2. Experimental data showing variables and bio-oil yield.

Run	Temp. (<i>I</i>) ($^{\circ}\text{C}$)	Heating rate (<i>J</i>) ($^{\circ}\text{C}/\text{min}$)	N_2 flowrate (<i>K</i>) (ml/min)	Yield of bio-oil (%)
1	650	15	2	47.93
2	550	15	4	57.03
3	350	10	2	42.70
4	650	5	4	45.69
5	550	15	6	59.03
6	450	5	8	50.67
7	350	15	4	43.77
8	550	5	2	50.69
9	350	15	2	43.75
10	650	10	2	46.43
11	350	5	4	40.53
12	650	15	4	48.93
13	450	10	4	52.83
14	550	20	2	55.03
15	650	5	4	45.93
16	550	20	4	55.93
17	450	10	6	52.90
18	650	10	2	46.00
19	350	15	4	43.04
20	550	15	8	56.93

$$n = 2^r + 2r + 6 \quad (4)$$

Considering the three independent variables ($r = 3$), a total of eight factorial points, six axial points, and six replications were obtained, resulting in a total of 20 experiments. The variables used and their levels are presented in Table 1, while the generated matrix of the CCD for the yield of the bio-oil is presented in Table 2. Linear, quadratic, and cubic model equations were tested using the experimental data to observe the effects of the individual variables and their interactions on the bio-oil yield.

Table 3. Physical and fuel properties of bio-oil produced at 590°C, 17°C/min heating rate, 6 ml/min N₂ flowrate, and 25 min.

Parameter	Value obtained
Fire point	97.0°C
pH	5.82
Flash point	72.8°C
API gravity	18.74
Density	0.961 g/ml
Kinematic viscosity @ 40°C	8.8 cSt

Table 4. Elemental content and heating values of the bio-oil produced at 590°C, 17°C/min heating rate, 6 ml/min N₂ flowrate, and 25 min.

Property	Value/unit
MC	19.5 wt%
Ash content	0.21 wt%
C	47.7 wt%
H	6.89 wt%
N	0.43 wt%
O	34.7 wt%
S	0.06 wt%
HHV	20.91 MJ/kg
LHV	19.41 MJ/kg

Table 5. Functional groups analysis of the bio-oil produced at 590°C, 17°C/min heating rate, 6 ml/min N₂ flowrate, and 25 min.

Adsorption band (cm ⁻¹)	Group	Compounds
3011.7	C-H stretching	Aromatic (phenyl ring)
2922.2	C-H stretching	Aliphatic (alkanes and alkenes)
2855.1	C-H stretching	Aliphatic (alkanes)
2668.8	C-H stretching	Aldehydes
1744.4	C=O stretching	Esters or ketones
1710.8	C=O stretching	Carbonyl compounds (aldehydes or ketones)
1461.1	C-H bending	Methyl groups
1379.1	C-H bending	Aromatic (phenyl group)
1282.2	C-H bending	Aliphatic (methylene groups)
1244.9	C-O stretching	Esters
1166.7	C-N stretching	Amines
935.6	C-H bending	Aromatic
834.9	C-H bending	Aromatic
805.1	C-H bending	Aliphatic
767.8	C-H bending	Aromatic
723.1	C-H bending	Aliphatic

The modelling and optimization of operating parameters involved a two-step process. First, a mathematical relationship between the bio-oil yield (response variable) and the independent variables (heating rate, temperature, and nitrogen flow rate) was established using Equation (5) [27, 29]:

$$y = f(x_1, x_2, x_3, \dots, x_n) \quad (5)$$

where f is an unknown function of the response, $x_1, x_2, x_3, \dots, x_n$ represent the independent factors, and n is the number of independent variables. Secondly, the coefficients of the mathematical model were estimated using a second-order equation, aiming to predict, optimize, and determine the main interaction factors (temperature, heating rates, and nitrogen flow rate) and their impact on the bio-oil yield. This is illustrated in Equation (6) [26, 30]:

$$y = \beta_0 + \sum_{i=1}^r \beta_i x_i + \sum_{i=1}^r \beta_{ii} x_i^2 + \sum_{i=1}^r \sum_{j=1}^r \beta_{ij} x_i x_j + \epsilon_i \quad (6)$$

where y represents the pyrolysis yield (dependent factor), x_i and x_j are the coded independent factors, $\beta_0, \beta_i, \beta_{ii}$, and β_{ij} are the coefficients of the linear, quadratic, and interaction effects, respectively, r is the number of independent factors, and ϵ_i is the random error. The model's performance was evaluated using analysis of variance (ANOVA).

3. Results and discussion

3.1 Results of characterization

3.1.1 Proximate and ultimate analysis results

The proximate analysis of elephant grass indicates a moisture content (MC) of $0.86 \pm 0.3\%$, a fixed carbon (FC) level of $14.22 \pm 0.4\%$, a volatile matter (VM) percentage of $79.24 \pm 0.4\%$, and an ash content of $5.86 \pm 0.1\%$. The high volatile matter content of the biomass can significantly influence its combustion characteristics and energy value since volatile matter content in biomass correlates with the luminous region and intensity during combustion, affecting flammability and calorific value [31]. The biomass also has a low ash content (5.86%). Biomass with low ash content exhibits better fuel properties, such as higher energy values and reduced emissions of volatile components, sulphur, and fly ash, thus contributing to a cleaner environment [32]. The

Table 6. Chemical composition of elephant grass bio-oil produced at 590°C, 17°C/min heating rate, 6 ml/min N₂ flowrate, and 25 min.

Peak	Retention time (min)	Area (%)	Compound	Quality
1	5.5363	0.3524	<i>o</i> -Xylene	97
2	5.6632	0.5282	Benzene, 1,3-dimethyl-	95
3	6.2916	0.6307	<i>o</i> -Xylene	90
4	6.6217	1.2747	Nonane	91
5	7.1421	0.4761	<i>cis</i> -Z-11,12-Epoxytetradecan-1-ol	43
6	7.3867	0.5857	Cyclohexanone, 2,3-dimethyl-	74
7	7.6859	0.6869	Nonane, 3-methyl-	70
8	7.8332	0.3839	Octane, 2,3-dimethyl-	47
9	7.9553	0.2869	Benzene, propyl-	55
10	8.1905	1.4564	Benzene, 1-ethyl-3-methyl-	95
11	8.4324	1.3056	Benzene, 1,2,4-trimethyl-	94
12	8.5336	0.572	Octane, 3,5-dimethyl-	76
13	8.6754	0.9309	Benzene, 1,2,3-trimethyl-	60
14	9.142	2.3282	Benzene, 1,2,3-trimethyl-	95
15	9.6797	2.6727	Decane	97
16	9.9275	0.6715	Benzene, 1,2,3-trimethyl-	95
17	10.4377	1.0392	Decane, 4-methyl-	90
18	10.5526	0.2635	Cyclohexane, (2-methylpropyl)-	74
19	10.8764	0.3112	Benzene, 1-methyl-3-propyl-	93
20	11.1036	0.5203	<i>o</i> -Cymene	94
21	11.7046	0.5899	Benzene, 2-ethyl-1,3-dimethyl-	86
22	11.8907	0.5224	Benzene, 4-ethyl-1,2-dimethyl-	95
23	12.4554	0.3783	Benzene, 1,4-diethyl-	41
24	12.8061	1.619	Undecane	96
25	12.9826	0.1764	Benzene, 1,2,4,5-tetramethyl-	97
26	13.3942	0.3731	1-Methyldecahydronaphthalene	97
27	13.727	0.2883	Cyclohexane, pentyl	80
28	14.6161	0.2132	Naphthalene	95
29	15.8424	0.3758	Dodecane	97
30	17.9191	0.1177	Naphthalene, 2-methyl	97
31	29.0147	0.1237	Methyl tetradecanoate	98
32	29.1553	0.0727	Heneicosane	91
33	30.174	0.0817	1-Octadecene	99
34	30.2918	0.0667	Octadecane	97
35	31.2117	0.0744	9-Hexadecenoic acid, methyl ester, (Z)-	99
36	31.345	0.0601	Nonadecane	98
37	31.4595	4.8357	Hexadecanoic acid, methyl ester	98
38	31.6606	0.1735	Octadecane	91
39	31.9392	6.8574	<i>n</i> -Hexadecanoic acid	99
40	32.0169	0.2724	Undecanoic acid, ethyl ester	90
41	32.1201	0.1341	1-Octadecene	97
42	32.1883	0.1202	Eicosane	96
43	32.2722	0.171	Heptadecanoic acid, methyl ester	95
44	32.5759	0.867	<i>n</i> -Hexadecanoic acid	93
45	32.7587	5.5054	9,12-Octadecadienoic acid, methyl ester	99
46	32.8212	5.4012	11-Octadecenoic acid, methyl ester	99
47	33.0034	2.2364	Methyl stearate	99
48	33.3459	48.9961	9,12-Octadecadienoic acid (Z,Z)-	98
49	33.6152	1.9226	9,12-Octadecadienoic acid (Z,Z)-	95
50	34.4749	0.0965	Methyl 18-methylnonadecanoate	96

Table 7. ANOVA for quadratic model.

Source	Sum of square	df	Mean square	F-value	P-value	
Model	395.67	9	43.96	7.32	.0023	Significant
I—Temperature	60.89	1	60.89	10.14	.0097	Significant
J—Heating rate	40.13	1	40.13	6.68	.0272	Significant
K—N ₂ flowrate	13.74	1	13.74	2.29	.1612	Not significant
IJ	44.79	1	44.79	7.46	.0211	Significant
IK	2.52	1	2.52	0.4198	.5316	Not significant
JK	176.44	1	176.44	29.39	.0003	Significant
I ²	45.32	1	45.32	7.55	.0206	Significant
J ²	0.2847	1	0.2847	0.0474	.8320	Not significant
K ²	17.53	1	17.53	2.92	.1183	Not significant
Residual	60.03	10	6.00			
Lack of fit	8.86	4	2.21	0.2597	.8936	Not significant
Pure error	51.17	6	8.53			
Cor Total	455.70	19				

Table 8. Model summary statistics.

Parameter	Value
Std. dev.	2.45
Mean	45.99
CV %	5.33
R ²	0.8683
Adjusted R ²	0.7497
Predicted R ²	0.7915
Adeq precision	12.0386

obtained ash content of the biomass is comparable to the range of ash content for woody (Afara and Iroko) and agricultural biomass species reported as 0.61%–5.03% and 3.25%–7.5%, respectively [33]. The volatile matter of the biomass (79.24%) is within the range reported in the literature [34–36].

The ultimate analysis of elephant grass reveals that the carbon (C) content is $45.44 \pm 0.1\%$, hydrogen (H) is $5.59 \pm 0.3\%$, nitrogen (N) is $0.67 \pm 0.2\%$, oxygen (O) is $40.95 \pm 0.1\%$, and sulphur (S) is $0.35 \pm 0.1\%$. The results show that elephant grass has a high carbon content (45.44%), which is favourable for bio-oil production. The hydrogen content (5.59%) and low nitrogen (0.67%) and sulphur (0.35%) contents are beneficial for producing high-quality bio-oil with minimal NO_x and SO_x emissions [37]. These results are consistent with findings from other biomasses [34, 38, 39]. This indicates that elephant grass is a reliable feedstock for bio-oil production.

3.1.2 Structural composition and heating value of biomass

The structural composition of the sample biomass consists of 46.28% cellulose, 29.90% hemicellulose, and 24.60% lignin. The cellulose and hemicellulose contents are slightly higher than the values reported by Wu *et al.* [40] for the same type of elephant grass. The relatively high value of the biomass's higher heating value (HHV) of 18.520 MJ/kg can be attributed to the low ash content and high carbon content of the biomass [41]. This composition, with a higher proportion of cellulose and hemicellulose, makes elephant grass a promising feedstock for bio-oil production due to its favourable energy content and structural properties.

3.2 Bio-oil characterization

3.2.1 Physico-chemical properties of bio-oil

The physical and fuel properties of the bio-oil derived from elephant grass are presented in Table 3, while the elemental analysis, higher heating value (HHV) and lower heating value (LHV) are shown in Table 4.

As shown in Table 4, the density of the bio-oil (0.961 g/ml) exceeds that of conventional fuel oil (0.920 g/ml) [42], classifying it as heavy oil. The kinematic viscosity of the bio-oil (8.8 cSt) differs significantly from values reported by Okoroigwe *et al.* [43] and Suchithra *et al.* [44], but aligns with findings by Sensoz and Angin [42]. This higher viscosity suggests the bio-oil is suitable for applications requiring heavy oil, such as fuel for furnaces, ships, and transformers [42]. The pH value (5.82) is higher than that reported by Chukwunke *et al.* [37] but falls within the range reported by other studies [45].

Table 4 presents the elemental content and heating values of the bio-oil derived from the study. The moisture content (MC) of 19.5 wt% indicates the presence of water in the composition, which is crucial for understanding its handling and storage requirements. The low ash content of 0.21 wt% suggests minimal inorganic residues, enhancing the bio-oil's purity for potential applications. The elemental composition includes 47.7 wt% carbon (C), 6.89 wt% hydrogen (H), 0.43 wt% nitrogen (N), 34.7 wt% oxygen (O), and 0.06 wt% sulphur (S). These elements play significant roles in determining the bio-oil's chemical properties and combustion characteristics. The HHV of 20.91 MJ/kg represents the maximum heat released during complete combustion, while the LHV of 19.41 MJ/kg accounts for the heat lost in vaporizing water in the combustion process. These properties underscore the bio-oil's potential as a renewable energy source with diverse industrial applications.

3.2.2 FTIR analysis of bio-oil

Table 5 presents the infrared spectrum of the bio-oil obtained from elephant grass pyrolysis, highlighting distinct absorbance peaks indicative of various functional groups.

The presence of specific chemicals identified through infrared spectroscopy in bio-oil obtained from elephant grass pyrolysis holds significant implications for its potential applications and industrial utility. Aliphatic hydrocarbons, such as alkenes and

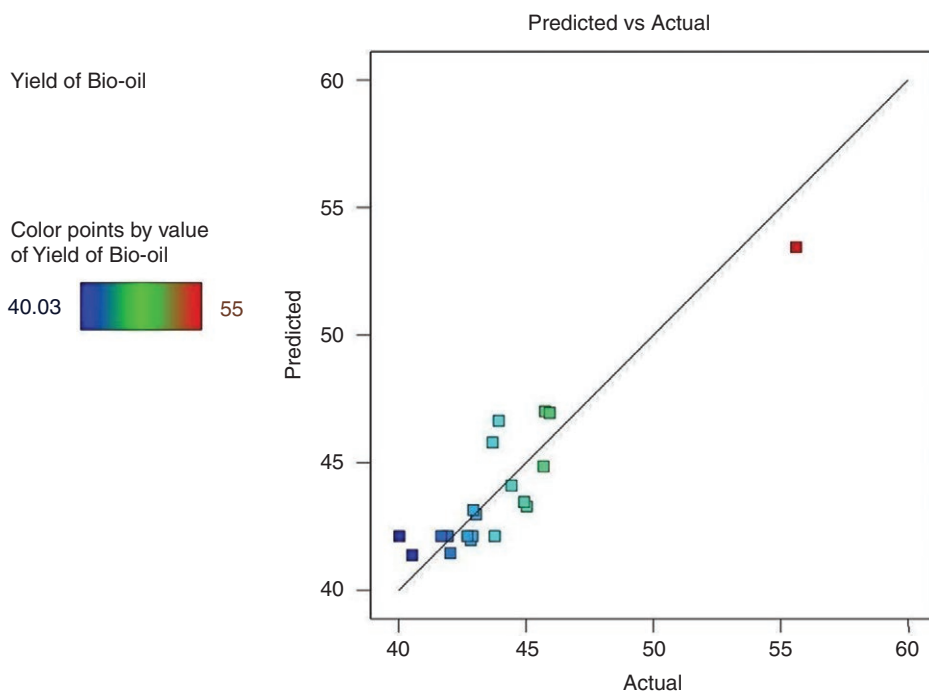


Figure 1. Plot of predicted vs actual experimental results.

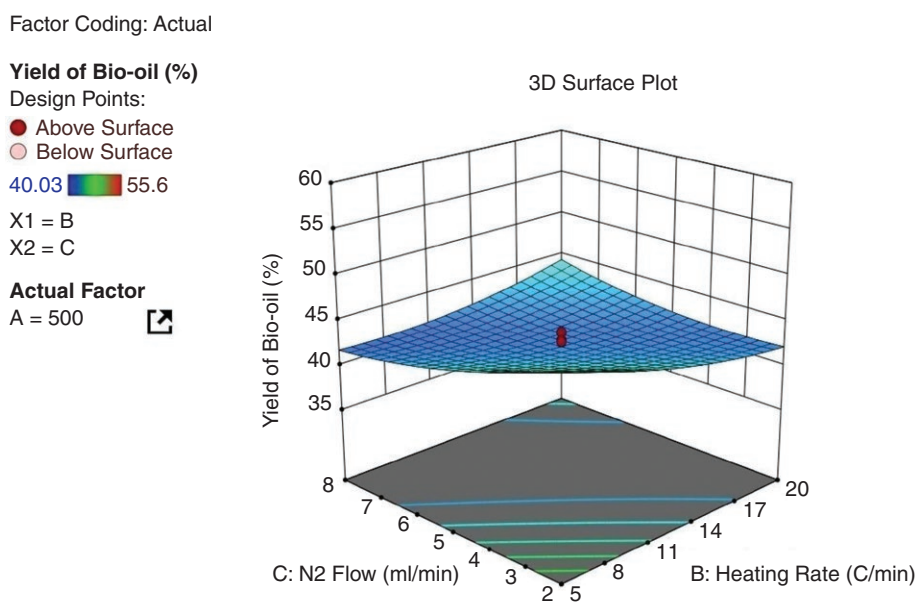


Figure 2. Plot of N2 flowrate and heating rate on 3D.

alkanes, identified by the absorption peak at 2922.2 cm^{-1} , are crucial as they contribute to the bio-oil's energy content and combustion properties [6, 37]. These compounds are desirable for fuel applications due to their high energy density and ability to burn efficiently. The presence of C=O stretching vibrations at 1703.4 cm^{-1} , indicating carboxylic acids and their derivatives like esters and aldehydes [46], suggests potential uses in the chemical industry. Carboxylic acids and esters contribute to the bio-oil's stability and viscosity characteristics. Aromatic compounds, identified by the absorption band at 1379.1 cm^{-1} corresponding to C=C stretching in aromatic rings [47], enhance the bio-oil's potential as a feedstock for specialty chemicals, including antioxidants,

dyes, and pharmaceuticals. Aromatic compounds can also improve the bio-oil's thermal stability and resistance to oxidation, extending its shelf life and application range.

3.2.3 Chemical analysis of bio-oil

Table 6 shows the result of the GC-MS analysis of the bio-oil.

The chemical composition analysis of the elephant grass bio-oil presented in Table 6 reveals a diverse array of chemical compounds. The bio-oil consists of various chemical groups including phenols, aldehydes, esters, hydrocarbons, and acids, as indicated by the identified compounds such as o-xylene, nonane, benzene derivatives, and fatty acid methyl esters [6, 37, 45, 48]. These

Factor Coding: Actual

Yield of Bio-oil (%)

Design Points:

● Above Surface

○ Below Surface

40.03  55.6

X1 = A

X2 = B

Actual Factor

C = 5 

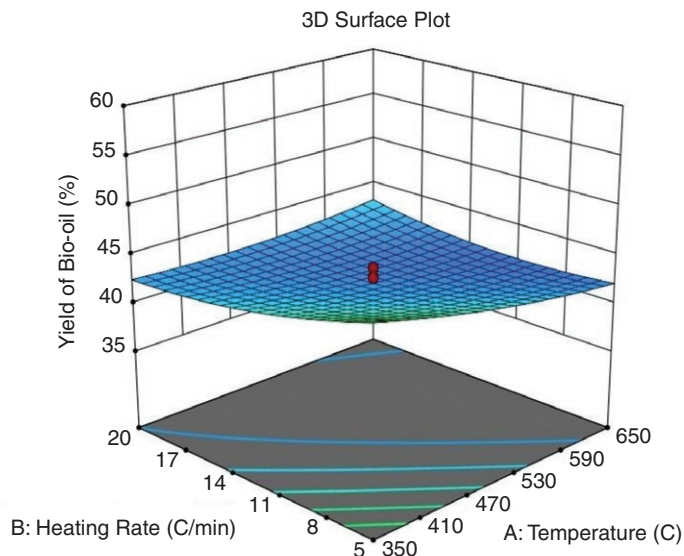


Figure 3. Plot of heating rate and temperature on 3D.

Factor Coding: Actual

Yield of Bio-oil (%)

Design Points:

● Above Surface

○ Below Surface

40.03  55.6

X1 = A

X2 = C

Actual Factor

B = 12.5 

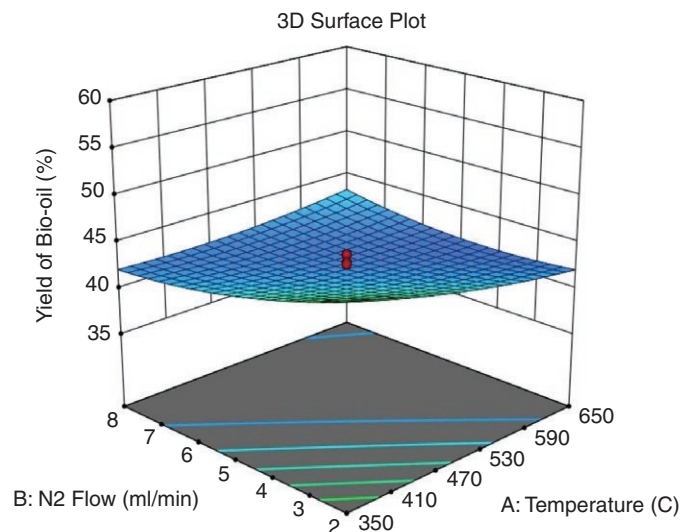


Figure 4. Plot of N2 flowrate and temperature on 3D.

Table 9. Model validation at optimum conditions.

Variables	Optimum values	Bio-oil yield (%)	
		Experimental	Predicted
Temperature A (°C)	590	59.03	55.60
Heating rate B (°C/min)	17		
Nitrogen flowrate (ml/min)	6		

findings reveal the complex nature of the bio-oil composition, which is typical in pyrolysis products of biomass [7]. The presence of these compounds suggests potential applications in biofuel

production and various industries [6], including chemicals and pharmaceuticals, to produce specialty chemicals such as resins, formaldehyde, and acetaldehyde.

3.3 Modelling the bio-oil yield

Table 7 presents the results of the ANOVA conducted to evaluate the adequacy of the multiple regression model used in this study.

Based on Table 5, the ANOVA results for the quadratic model applied in this study are presented. The model itself shows a significant fit (F -value = 7.32, P = .0023), indicating that the selected quadratic terms adequately explain the variation in the response variable. Among the individual factors, temperature (I), and heating rate (J) exhibit significant effects (P < .05), influencing the response positively. Conversely, the N_2 flow rate (K) does not significantly impact the response (P = .1612). The interactions IJ and JK are also significant (P < .05), highlighting their combined influence on the response variable. Non-significant terms include IK , J^2 , and K^2 (P > .05), suggesting their negligible contribution. The lack of fit test confirms that the model fits well (P = .8936), supporting its adequacy for predicting the response variable under the experimental conditions studied. The final mathematical equation is shown in Equation (7).

$$\text{Bio-oil yield} = 42.13 + 1.14I + 0.9459J + 1.46IJ + 2.26JK + 0.621I^2 \quad (7)$$

Table 8 shows the model summary statistic for the bio-oil yield. Table 8 provides summary statistics for the model. The low standard deviation (2.45) indicates consistent predictions with minimal variability around the mean (45.99). A coefficient of variation (CV %) of 5.33% suggests stable predictions closely clustered around the average. The R^2 value of 0.8683 indicates that the model explains 86.83% of the variability in the dependent variable, demonstrating strong explanatory power. The high predicted R^2 (0.7915) suggests the model's ability to generalize well to new data. Figure 1 illustrates the predicted versus actual experimental results, further validating the model's performance.

Comparing the results predicted by the mathematical model with the experimental results, as depicted in Fig. 1, reveals a uniform distribution of errors. This consistency across the range of predictions indicates that the model effectively captures the underlying relationships in the data [12]. The plot demonstrates that the discrepancies between predicted and actual values are evenly spread across the dataset, without any systematic biases or trends. This validation highlights the robustness of the model in accurately forecasting experimental outcomes, reinforcing its reliability and applicability in practical scenarios.

3.4 Parameter optimization

The 3D response surface plots of the elephant grass-derived bio-oil yield are shown in Figs 2–4.

Figure 2 illustrates the relationship between nitrogen flow rate (NFR) and heating rate (HR) on bio-oil yield. The highest yield of bio-oil (49%) was achieved at 8 ml/min NFR and 20°C/min HR. Increasing both NFR and HR led to an observable increase in bio-oil yield. This trend can be explained by the reduction in residence time, which prevents tar formation, enhances volatile matter release from biomass, and minimizes secondary reactions, thereby promoting optimal bio-oil formation.

Figure 3 shows the combined effect of heating rate and temperature on bio-oil yield. It demonstrates that higher heating rates and temperatures synergistically enhance bio-oil yield within the investigated ranges. Faster heating rates reduce residence time, which is beneficial for minimizing secondary reactions and improving the conversion of biomass into bio-oil. Elevated temperatures facilitate the thermal decomposition of complex organic compounds, leading to increased production of volatile components essential for bio-oil formation.

Figure 4 explores the impact of nitrogen flow rate and temperature on bio-oil yield and residence time. It indicates that increasing nitrogen flow rate and temperature enhances bio-oil yield. Higher temperatures promote bio-oil yield by facilitating the breakdown of complex organic compounds, while increased nitrogen flow rates reduce residence time, thereby minimizing exposure to high temperatures and reducing non-bio-oil product formation due to secondary reactions.

3.5 Validation of model

The validity of the model was further confirmed by performing three sets of parallel tests using the optimum values, and the mean values were recorded. The variables tested include a temperature of 590°C, a heating rate of 17°C/min, and a nitrogen flow rate of 6 ml/min. The results are presented in Table 9.

As shown in Table 9, the experimental bio-oil yield at the optimum conditions was 59.03%, closely aligning with the model's predicted yield of 55.60%. This close agreement between experimental and predicted values indicates that the model is reliable and can accurately predict bio-oil yields under the specified conditions.

4. Conclusion

The investigation into elephant grass lignocellulose biomass demonstrates its potential for biofuel production. Its physicochemical characteristics are comparable to those of other lignocellulosic biomasses, supporting its viability for bio-oil production through pyrolysis. A factorial model using nitrogen flow rate, heating rate, and temperature was developed, with ANOVA analysis confirming its reliability. Optimal conditions yielded a bio-oil yield of 59.03 wt%, closely matching predicted values, highlighting the model's robustness. The derived bio-oil is suitable for various heating systems, showcasing its practical applications. This research considered elephant grass samples from a specific geographic region; however, geographic and environmental factors may likely affect the properties of the elephant grass, which in turn can influence both bio-oil yield and quality. Future research should assess the impact of geographic and environmental factors on elephant grass and refine the model to include co-products for a more comprehensive understanding of the pyrolysis process. Moreover, the laboratory-based findings may not accurately reflect real-world conditions, emphasizing the need for larger-scale experiments and region-specific studies to validate and enhance the applicability of the results across diverse contexts. While ANOVA has confirmed the model's reliability, increasing the sample size and incorporating additional variables could further strengthen the statistical analysis.

Author contributions

Sunday Ikpeseni (Conceptualization [equal], Data curation [equal], Methodology [equal], Project administration [equal], Supervision [equal], Visualization [equal], Writing—original draft [equal], Writing—review & editing [equal]), Samuel Sada (Conceptualization [equal], Methodology [equal], Software [equal], Writing—original draft [equal]), Ufuoma Efebor (Conceptualization [equal], Data curation [equal], Formal analysis [equal], Methodology [equal], Software [equal], Visualization [equal], Writing—original draft [equal]), Henry Orugba (Conceptualization [equal], Data curation [equal], Methodology [equal], Resources [equal], Validation [equal], Writing—original

draft [equal]), Mathias Ekpu (Conceptualization [equal], Formal analysis [equal], Investigation [equal], Methodology [equal]), Hilary Owamah (Formal analysis [equal], Methodology [equal], Project administration [equal], Supervision [equal], Writing—original draft [equal], Writing—review & editing [equal]), Jeremiah Chukwunke (Methodology [equal], Software [equal], Validation [equal], Visualization [equal], Writing—original draft [equal]), Solomon Onyebisi (Software [equal], Validation [equal], Writing—review & editing [equal]), and Uche Onochie (Formal analysis [equal], Visualization [equal], Writing—original draft [equal])

Conflict of interest statement

This is to inform you that this manuscript titled “Response Surface Methodology (RSM) Optimization of Bio-oil derived from Pyrolysis of Elephant grass” contains original work done by the authors. The authors have no conflict of interest with any other and have submitted this manuscript to your journal house for possible publication. The manuscript has neither been submitted to this journal before nor any other journal.

Funding

The research was self-funded by the authors.

Data availability

Data will be made available by the corresponding author (scikpeseni@delsu.edu.ng) upon reasonable request.

References

- [1] Achebe CH, Onokpita E, Onokwai AO. Anaerobic digestion and co-digestion of poultry droppings (PD) and cassava peel (CP): comparative study of optimal biogas production. *J Eng Appl Sci* 2018;**12**:87–93.
- [2] Orugba HO, Ogbeide SE, Osagie C. Emission trading scheme and the effect of carbon fee on petroleum refineries. *Asian J Appl Sci* 2019;**7**:537–45.
- [3] Poornima S, Manikandan S, Prakash R et al. Biofuel and biochemical production through biomass transformation using advanced thermochemical and biochemical processes – a review. *Fuel* 2024;**372**:132204. <https://doi.org/10.1016/j.fuel.2024.132204>
- [4] Jahiril MI, Rasul MG, Chowdhury AA et al. Biofuels production through biomass pyrolysis – a technological review. *Energies* 2012;**5**:4952–5001. <https://doi.org/10.3390/en5124952>
- [5] Gao Y, Gao X, Zhang X. The 2 °C global temperature target and the evolution of the long-term goal of addressing climate change—from the United Nations Framework Convention on Climate Change to the Paris Agreement. *Engineering* 2017;**3**:272–8. <https://doi.org/10.1016/j.eng.2017.01.022>
- [6] Chukwunke JL, Orugba HO, Olisakwe HC et al. Pyrolysis of pig-hair in a fixed bed reactor: physico-chemical parameters of bio-oil. *S Afr J Chem Eng* 2021;**38**:115–20. <https://doi.org/10.1016/j.sajce.2021.09.003>
- [7] Orugba HO, Chukwunke JL, Olisakwe HC et al. Multi-parametric optimization of the catalytic pyrolysis of pig hair into bio-oil. *Clean Energy* 2021;**5**:527–35. <https://doi.org/10.1093/ce/zkab038>
- [8] Landrat M, Abawalo MT, Pikoń K et al. Bio-oil derived from Teff Husk via slow pyrolysis process in fixed bed reactor and its characterization. *Energies* 2023;**15**:9605. <https://doi.org/10.3390/en15249605>
- [9] Lachos-Perez D, Martins-Vieira JC, Missau J et al. Review on biomass pyrolysis with a focus on bio-oil upgrading techniques. *Analytica* 2023;**4**:182–205. <https://doi.org/10.3390/analytica4020015>
- [10] Prasetiawan H, Fardhyanti DS, Fatrisari W et al. Preliminary study on the bio-oil production from multi feed-stock biomass waste via fast pyrolysis process. *J Adv Res Fluid Mech Therm Sci* 2023;**103**:216–27. <https://doi.org/10.37934/arfm.103.2.216227>
- [11] Chukwunke JL, Sinebe JE, Orugba HO et al. Production and physico-chemical characteristics of pyrolyzed bio-oil derived from cow hooves. *Arab J Basic Appl Sci* 2022;**29**:363–71. <https://doi.org/10.1080/25765299.2022.2129633>
- [12] Orugba HO, Okechukwu OD, Njoku NC et al. Process modeling of sulphuric acid leaching of iron from Ozoro Clay. *Eur Sci J* 2014;**9**:76–9.
- [13] Orugba HO, Onukwuli OD, Babayemi AK et al. Five-factor response surface optimisation of hydrochloric acid dissolution of alumina from a Nigerian Clay. *Arid Zone J Eng* 2020;**16**:821–32.
- [14] Orugba HO, Edomwonyi-Otu LC. Improving the activity and stability of turtle shell-derived catalyst in alcoholysis of degraded vegetable oil: an experimental design approach. *J King Saud Univ Eng Sci* 2021;**35**:297–303. <https://doi.org/10.1016/j.jksues.2021.05.001>
- [15] Balamurugan S, Seenivasan D, Rai R et al. Optimization of biodiesel production process for mixed nonedible oil (processed dairy waste, mahua oil, and castor oil) using response surface methodology. *Proc Inst Mech Eng, Part E* 2022;**238**:862–74. <https://doi.org/10.1177/09544089221147392>
- [16] Oyeibanji JA, Okekunle PO, Itabiye OE. Box Behnken design application for optimization of bio-oil yield from catalytic pyrolysis of agro-residue. *Fuel Communications* 2023;**16**:100091. <https://doi.org/10.1016/j.fueco.2023.100091>
- [17] Onokwai AO, Okokpujie IP, Ajisegiri ESA et al. Application of response surface methodology for the modelling and optimisation of bio-oil yield via intermediate pyrolysis process of sugarcane bagasse. *Adv Mater Process Technol* 2023. <https://doi.org/10.1080/2374068x.2023.2193310>
- [18] Jeeru LR, Abdul FK, Anireddy JS et al. Optimization of process parameters for conventional pyrolysis of algal biomass into bio-oil and bio-char production. *Chem Eng Process* 2023;**185**:109311. <https://doi.org/10.1016/j.cep.2023.109311>
- [19] Fombu AH, Ochonogor AEC, Olayide OE. Use of response surface methodology in optimizing the production yield of bio-fuel from cashew nut shell through the process of pyrolysis. *IOP Conf Ser Earth Environ Sci* 2023;**1178**:012017. <https://doi.org/10.1088/1755-1315/1178/1/012017>
- [20] Irfan M, Ghalib SA, Waqas S et al. Response surface methodology for the synthesis and characterization of bio-oil extracted from biomass waste and upgradation using the Rice Husk Ash catalyst. *ACS Omega* 2023;**20**:17869–79. <https://doi.org/10.1021/acsomega.3c00868>
- [21] Oliveira L, Oliveira F, Silva G et al. Nitrogen and phosphorus fertilizer application to Elephant grass (*Cenchrus purpureus* syn. *Pennisetum purpureum*) cultivar ‘Cameroon’ in an arenosol in Rio Grande do Norte, Brazil. *Trop Grassl* 2022;**10**:280–7. [https://doi.org/10.17138/tgft\(10\)280-287](https://doi.org/10.17138/tgft(10)280-287)
- [22] Batista J, Alves D, Rigueira J et al. Elephant grass cv. BRS capiaçu silage with inclusion of different proportions of silk cotton. *Semin Cienc Agrar* 2022;**43**:179–96. <https://doi.org/10.5433/1679-0359.2022v43n1p179>

- [23] Ikpeseni SC, Orugba HO, Efetobor UJ et al. Pyrolysis characteristics and kinetics of the thermal degradation of elephant grass (*Pennisetum purpureum*): a comparative analysis using the Flynn–Wall–Ozawa and the Kissinger–Akahira–Sunose methods. *Environ Dev Sustain* 2023. <https://doi.org/10.1007/s10668-023-04322-6>
- [24] Wang F, Shi D, Han J et al. Comparative study on pretreatment processes for different utilization purposes of switchgrass. *ACS Omega* 2020;**5**:21999–2007. <https://doi.org/10.1021/acsomega.0c01047>
- [25] Ohimain EI, Kendabie P, Nwachukwu RES. Bioenergy potentials of elephant grass, *Pennisetum Purpureum* S. *Annu Res Rev Biol* 2022;**4**:2215–27.
- [26] Hossain MA, Ganesan P, Jewaratnam J et al. Optimization of process parameters for microwave pyrolysis of Oil palm fiber (OPF) for hydrogen and biochar production. *Energy Convers Manage* 2017;**133**:349362. <https://doi.org/10.1016/j.enconman.2016.10.046>
- [27] Isahak WNRW, Hisham MWM, Yarmo MA et al. A review on bio-oil production from biomass by using pyrolysis method. *Renew Sustain Energy Rev* 2012;**16**:5910–23. <https://doi.org/10.1016/j.rser.2012.05.039>
- [28] Onarheim K, Hannula I, Solantausta Y. Hydrogen enhanced biofuels for transport via fast pyrolysis of biomass: a conceptual assessment. *Energy* 2020;**199**:117337. <https://doi.org/10.1016/j.energy.2020.117337>
- [29] Laouge ZB, Çiğgin AS, Merdun H. Optimization and characterization of bio-oil from fast pyrolysis of Pearl Millet and *Sidacordifolia* L. by using response surface methodology. *Fuel* 2020;**274**:117842. <https://doi.org/10.1016/j.fuel.2020.117842>
- [30] Sada SO, Achebo J. Optimization and prediction of the weld bead geometry of a mild steel metal inert gas weld. *Adv Mater Process Technol* 2022;**8**:1625–34. <https://doi.org/10.1080/2374068x.2020.1860597>
- [31] Jia Y, Li Z, Wang Y et al. Visualization of combustion phases of biomass particles: effects of fuel properties. *ACS Omega* 2021;**6**:27702–10. <https://doi.org/10.1021/acsomega.1c02783>
- [32] Dalkhsuren D, Iwabuchi K, Itoh T et al. Effects of ash composition and combustion temperature on reduced particulate matter emission by biomass carbonization. *Bioenergy Res* 2023;**16**:1629–38. <https://doi.org/10.1007/s12155-022-10526-x>
- [33] Ogunsola OE, Adeleke O, Aruna AT. Wood fuel analysis of some selected wood species within Ibadan. *IOP Conf Ser Earth Environ Sci* 2018;**173**:012043. <https://doi.org/10.1088/1755-1315/173/1/012043>
- [34] Balogun AO, Lasode OA, Mcdonald AG. Devolatilisation kinetics and pyrolytic analyses of *Tectona grandis* (Teak). *Bioresour Technol* 2014;**156**:57–62. <https://doi.org/10.1016/j.biortech.2014.01.007>
- [35] Yang W, Fu P, Yi WM. Catalytic fast pyrolysis of corn stover in a fluidized bed heated by hot flue gas: Physicochemical properties of bio-oil and its application. *Int J Agric Biol Eng* 2017;**10**:226–33.
- [36] Oyebanji JA, Okekunle PO, Oyedepo SO et al. Physicochemical properties of wood sawdust: a Preliminary study. *IOP Conf Ser Mater Sci Eng* 2021;**1107**:012125. <https://doi.org/10.1088/1757-899x/1107/1/012125>
- [37] Chukwunke JI, Chukwujike IC, Okolie PC. Physico-chemical analysis of pyrolyzed bio-oil from *Swietenia macrophylla* (Mahogany) wood. *Heliyon* 2019;**5**:e1790. <https://doi.org/10.1016/j.heliyon.2019.e01790>
- [38] Srivastava N, Shrivastav A, Singh R et al. Advances in the structural composition of biomass: fundamental and bioenergy applications. *J Renewable Mater* 2021;**9**:615–36. <https://doi.org/10.32604/jrm.2021.014374>
- [39] Garcia JC, Alfaro A, Loaiza JM. Cold alkaline extraction of elephant grass for optimal subsequent extraction of hemicelluloses and energy production. *Biomass Convers Biorefin* 2022;**14**:8307–20. <https://doi.org/10.1007/s13399-022-03054-3>
- [40] Wu L, Zhang J, Xue X et al. Hydrocarbon-Rich bio-oil production from catalytic pyrolysis of biomass over the undervalued ZSM-11 zeolites. *ACS EST Eng* 2022;**2**:670–80. <https://doi.org/10.1021/acsestengg.1c00329>
- [41] Balogun AO, Lasode OA, Onokwai AO et al. Elemental analysis and combustion characteristics evaluation of Nigeria biomass resources. *Int J Mec Eng Technol* 2019;**10**:1522–7.
- [42] Sensoz S, Angin D. Pyrolysis of Safflower (*Charthamus tinctorius* L) seed press cake: Part 1. The effects of pyrolysis parameters on the product yields. *Bioresour Technol* 2008;**99**:5492–7. <https://doi.org/10.1016/j.biortech.2007.10.046>
- [43] Okoroigwe E, Zhengong L, Stuecken T et al. Pyrolysis of *Gmelina arborea* wood for bio-oil/bio-char production: physical and chemical characterization of product. *J Appl Sci* 2012;**12**:369–74. <https://doi.org/10.3923/jas.2012.369.374>
- [44] Suchithra T, Sushil A, Harideepan R et al. Physicochemical properties of bio-oil produced at various temperatures from pine wood using an auger reactor. *Bioresour Technol* 2010;**101**:8389–95. <https://doi.org/10.1016/j.biortech.2010.05.040>
- [45] Oyebanji JA, Ololade ZS. Fast pyrolysis of *Tectona grandis* wood for bio-oil characterization and bactericidal potentials. *Glob J Res Eng* 2017;**17**:15–22.
- [46] Pinto O, Romero R, Carrier M et al. Fast pyrolysis of tannins from pine bark as a renewable source of Catechols. *J Anal Appl Pyrolysis* 2018;**136**:69–76. <https://doi.org/10.1016/j.jaap.2018.10.022>
- [47] Idowu AA, Ogunsanwo OY, Ayodeji RI. Bio-fuel properties and elemental analysis of bio-oil produced from pyrolysis of *Gmelina arborea*. *Acta Chem Malaysia* 2020;**5**:38–41. <https://doi.org/10.2478/acmy-2021-0006>
- [48] Kim E, Gil H, Park S et al. Bio-oil production from pyrolysis of waste sawdust with catalyst ZSM-5. *J Mater Cycles Waste Manage* 2017;**19**:423–31. <https://doi.org/10.1007/s10163-015-0438-z>